ANNEXE I

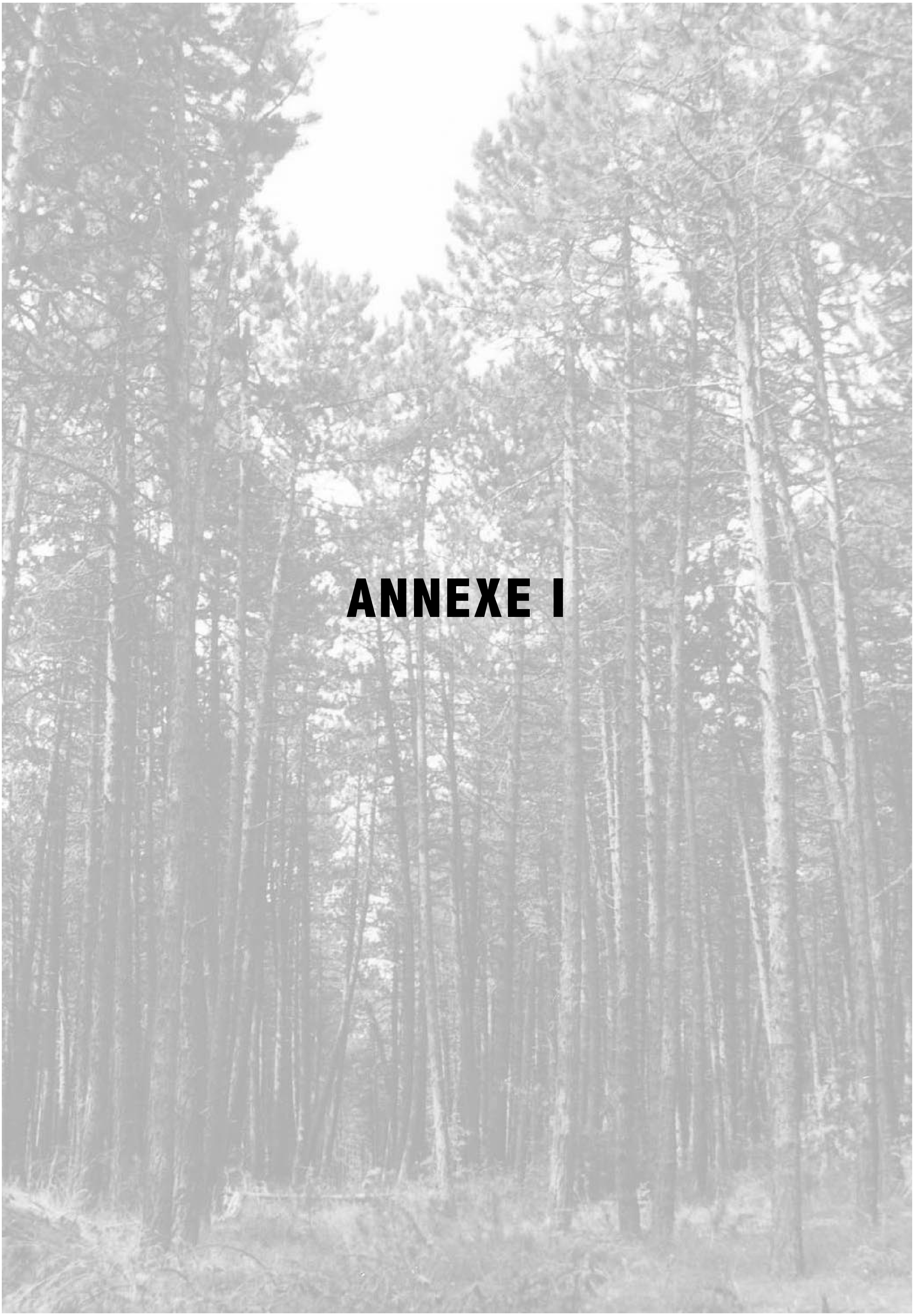

Etude du potentiel de l'interférométrie radar pour la foresterie.

« ERS INSAR data for remote sensing over hilly forested areas »

T. Castel, J.M. Martinez, A. Beaudoin, U. Wegmuller, T. Strozzi

Remote Sensing Environment, Juillet 2000, p 73-86.

ERS INSAR DATA FOR REMOTE SENSING HILLY FORESTED AREAS

Thierry Castel[1,*,‡]

[1]LCT Cemagref-ENGREF, 500 rue J.F. Breton, 34093 Montpellier Cedex 05 - France

*Now with CIRAD-amis, Programme Modélisation des Plantes
Current address: Université de Bourgogne, CRC UMR 5080 CNRS, 6 Bd. Gabriel
Bât. Sciences Gabriel, 21004 Dijon Cedex - France
Fax: +33. 3.80.39.57.41 e-mail: Thierry.Castel@u-bourgogne.fr

Jean-Michel Martinez[1,**]

**Now with Centre d'Etudes Spatiales de la Biosphère (CESBIO)
Bpi 2801 18 avenue E. Belin 31055 Toulouse Cedex 4 - France
Fax: +33 5.61.55.85.00 e-mail: Jeanmichel.Martinez@cesbio.cnes.fr

André Beaudoin[1,***]

*** Now with Aerospace and Navigation Radar Section /Defence Research Establishment
3701 Carling Avenue Bldg T86, Ottawa, Ontario K1A 0K2 - Canada

Urs Wegmüller, Tazio Strozzi

Gamma Remote Sensing, Thunstrasse 130, CH-3074 Muri b. Bern, Switzerland
Fax: +41(0). 31-951.70.08 email: strozzi@gamma-rs.ch

In press
Remote Sensing of Environment
December 99

‡ To whom proofs and correspondence should be sent.

Abstract

ERS INSAR data have been proved to be of interest for forest applications. The interferometric coherence was found related to various land-uses and forest types, whereas in some special cases (e.g. flat terrain) the interferometric phase has been linked to the forest height. This paper reports an investigation on the information content of the interferometric coherence over a hilly terrain supporting various land-uses types and large pine plantations. The approach includes the use of a Geographic Information System and multi-temporal data to analyze the coherence behavior as a function of forest types forest parameters and environmental factors such as meteorological and topographic effects.

Coherence appears to be efficient to discriminate between forest types. However topography and environmental conditions affects strongly the coherence and its estimation, pointing out the need for rejection of strong slopes areas (> 15°) and the sensitivity to local meteorological/seasonal effects. Based on these observations, forest classification results are presented. Forest/non-forest discrimination is very efficient (accuracy > 90%) using one-day interval acquisition. More detailed classification with discrimination between forest themes gives also good results.

Then, we investigate the indirect link between coherence and forest parameters. The coherence is sensitive to the forest growth stage allowing forest parameters retrieval possible using a simple straight-line model.. Finally, the importance of wind upon temporal deccorelation is addressed, and a semi-empirical correction is proposed.

Keywords: ERS differential interferometry, coherence, forest, classification, biomass retrieval, topography, meteorology.

1 Introduction

Space-borne Synthetic Aperture Radars (SARs) data have shown a great potential for forest applications including mapping and biomass retrieval over flat and hilly terrain (Beaudoin et al., 1994; Beaudoin et al., 1995; Dobson et al., 1995; Ranson et al., 1995). However, studies using ERS SAR data showed that its configuration is somewhat limited for forest applications (Dobson et al., 1992; Kasischke et al., 1994; Wang et al., 1994). In addition to low-level cover discrimination such as forest/non-forest mapping, possible applications are mainly related to the monitoring of natural or man-made forest perturbations such as clear-cutting (tropical deforestation), re-growth (low biomass levels) and environmental changes (e.g. thaw/freeze events).

Fortunately, applications can be broadened significantly when interferometric phase and correlation derived from repeat-pass ERS SAR interferometry (INSAR) data are considered, in addition to the usual backscatter information. The interferometric correlation (here after called degree of coherence), which is an indicator of the temporal stability of the target in terms of geometric properties, proved to be a good discrimination in cultivated areas (Wegmüller and Werner, 1995b) and forested landscapes (Herland, 1995; Wegmüller and Werner, 1995a), in particular when multi-pairs correlation are used (Wegmüller and Werner, 1997).It has been showed that the interferometric phase, usually used to derive the terrain altitude, can also be linked to the height of the forest canopy (Hagberg et al., 1995; Ulander et al., 1995; Askne et al., 1997; Floury et al., 1997). Furthermore, some studies have showed the potential of degree of coherence for forest parameters retrieval (Floury et al., 1996; Askne et al., 1997). Gens and van Genderen (1996) have recently listed a wide range of such applications, with encouraging results. However, these are recent results and the potential of such new data type is far from being fully explored. The interferometric, topographic and environmental conditions, for which INSAR data can provide useful thematic applications, have to be assessed furthermore.

In this paper, we address the potential use of ERS INSAR coherence data over hilly terrain, towards the generalization of 1) land-use mapping and especially detection of forested areas and 2) retrieve forest types and relevant forest parameters (e.g. stem biomass). This study differs somewhat from those previously reported about INSAR observations of forested areas. The approach consists in using multi temporal data and a Geographic Information System (GIS) to analyze the influence upon interferometric coherence of various factors such as time interval between acquisitions, biophysical parameters, meteorological/seasonal effects and topography.

The first part presents the test site and the associated data collection and processing. The second section investigates the general behavior of the degree of coherence for various land-uses and forest types over hilly terrain as well as the temporal instability of the signatures. In this section, we examine coherence capability for forest mapping using tandem data. The last part focuses on the retrieval of forest parameters, studying the indirect link between the coherence and the growth stage. In particular we focus on the influence of wind upon temporal decorrelation.

2 Test site and data-set

2.1 The test-site

The test-site is situated in the *Département de la Lozère*, in Southern France. This site presents a great interest because of the variability in forest types and topographic conditions. It is centered approximately at 44.5°30.0’ N and 0°3.5' E. The west part of the area is characterized by large and gently rolling limestone plateaus culminating around 1200 m, which are intersected by gorges with 300-500m depth and steep slopes up to 50° (see DEM in Figure 1). In the east part, there are the *Cévennes* mountains, with a mean altitude of about 800 m. The overall area is dominated by the *Mont-Lozère* (1660 m) with gentle slopes aligned along a east-west axis. Main land-uses are natural short grasslands. Cultivated and urban areas are concentrated in the valleys whereas on the plateaus Austrian and Scots pine plantations are found. Coniferous species such as spruce, Scots pine, fir and Douglas fir, but also deciduous species such as beech and chestnut trees mainly cover the rest of the scene.

Following, we focus on Austrian black pine plantations (*Pinus nigra nigricans)* which are found in state-owned forest plantations made of even-aged and relatively homogeneous stands. The two main forest test-sites (Figure 1) cover respectively 5400 and 1200 ha with more than 500 stands (average area 5-15 ha), offering a large range of growth stages (0 to 140 year-old) as well as topographic situations.

Different ground data concerning land-uses and these stands have been collected and entered in a Geographic Information System (GIS) that includes:

- a digital forest inventory (French forest inventory service IFN) covering the whole test-site (50 by 80 km) with a 50 meter grid size, in which more than 30 forested themes are described, defining the stands in terms of species and structure (sparse, reforestation, copse, young, mature,);
- a Digital Elevation Model (DEM) with a 50 meter grid size (French Geographic Institute IGN) with a 2.5 meter of vertical accuracy;
- stand limits and age classes of the Austrian pine plantations (> 500 stands);
- detailed measurements of forest parameters in 103 Austrian pine stands including mean height, basal area, stem density .From there, the stem volume is derived in a simple way by combining these parameters with a trunk taper factor. Then, the stem biomass can be

estimated by applying a dry wood density coefficient found to be equal to 360 kg/m^3 from measurements (Castel, 1998).

2.2 INSAR acquisition and processing

Principal INSAR products are contained in the normalized complex cross-correlation, which is defined as:

$$\rho \cdot e^{j\phi} = \frac{\langle s_e s_m^* \rangle}{\sqrt{\langle s_e s_e^* \rangle \langle s_m s_m^* \rangle}} \tag{1}$$

where ϕ is the interferometric phase (i.e. phase difference between the complex pixel values $s_{e,m}$ of slave and master images) and ρ is the degree of coherence. The brackets denote the ensemble average found by coherently averaging the complex values of N single look pixels, which means that the coherence is the measure of the spatial variability of the interferometric phase. The degree of coherence provides a measure of the stability of the phase difference between the two images and takes limited value in the range [0-1].

The decorrelation sources can be separated in three main origins (Zebker and Villasenor, 1992; Askne et al., 1997):

$$\rho_{total} = \rho_{thermal} \cdot \rho_{spatial} \cdot \rho_{temporal} \tag{2}$$

The thermal noise decorrelation $\rho_{thermal}$ can be neglected in the case of ERS data (Hagberg et al 1993, Askne et al., 1997). The spatial decorrelation $\rho_{spatial}$ due to the baseline was compensated with common-band filtering. For flat terrain it can be neglected because the interferograms we will study present baselines smaller than 150 meters. However, with volume scattering, in particular with large trees, the effective footprint size in range is increased. As the length of the range footprint projected normal to the range direction (in the imaging plane) is larger, then the resulting ‘celestial footprint’ is smaller and the coherence should decrease. However, this latter phenomenon won't be address in this paper considering that further theoretical modeling would be necessary to include this effect in our work.. Finally, the decorrelation is almost due to $\rho_{temporal}$ which is mainly an indicator of the temporal unstability of the target geometric and dielectric properties (Wegmüller and Werner, 1995b).

We analyzed 8 ERS interferograms (Table 1) including 4 tandem pairs which are two images of the same area acquired with one day interval by the ERS-1&2 satellites. The various acquisition parameters that must be accounted for in the analysis are presented in Table 1. We chose only pairs with relatively small baselines to prevent from excessive spatial decorrelation. Ignoring the tandem pair, it can be seen that the time acquisition interval is large, providing contrasted seasons and thus, variability in ground, forest and weather conditions. In particular, near-freezing conditions with a shallow snow layer on the ground were present for one winter scene included in pairs cp2-3 & cp3-5. Low wind conditions (i.e. from 10 to 30 km/h) prevailed for all pairs.

Tandem analysis was performed using Gamma's SAR and interferometric processing software (Strozzi et al., 1998) for the European program EUFORA (European Forest Observation by Radar), whereas the others interferograms were previously performed using the DIAPASON estimator (Massonnet, 1994) developed by the Centre Nationale d’Etudes Spatiales (CNES), under CNES contract.

The Gamma SAR processing included radiometric calibration for the antenna gain and slant range distance. For the interferometric processing the images were co-registered at sub-pixel accuracy and common band filtering of the azimuth and range spectra was applied in order to optimize the interferometric correlation and to minimize the effects of the baseline geometry on the degree of coherence. The true pixel size of the SAR data was computed from the DEM and the backscattering intensities were normalized. For the estimation of the terrain-corrected degree of coherence, a simulated unwrapped phase image in SAR coordinates was calculated from the DEM. The simulated phase image, which corresponds to the topographic phase, was then subtracted from the interferometric phase. From the differential interferogram and the two intensity images, the multi-look interferometric signatures were computed. For a wide applicability, the degree of coherence, the average backscatter intensity, and the backscattering intensity change between the two images of the Tandem pair were estimated on a per pixel level. In order to get reliable values at the pixel level and to find a compromise between maintaining a high spatial resolution and obtaining an accurate estimation, adaptive estimators and filtering were used (Wegmüller et al., 1998). In a final step, the DEM was used to transform the images from SAR coordinates to orthonormal map coordinates, permitting the validation of the forest map against the available land-use inventory.

The DIAPASON differs from the GAMMA Software in the way the coherence is estimated (Massonnet and Rabaute, 1993), which leads usually to slightly higher values than with GAMMA software. As a consequence the direct comparison of the results of the two estimators is not possible.

3 Results and discussion

3.1 Mapping forest

3.1.1 Degree of coherence potential for forest types discrimination.

In this section, we use the digital forest inventory and the DEM to study the sensitivity of the coherence to different factors such as tree species, meteorology and topography. In order to intersect these informations, we cross the images and the other information layers through the

GIS. Then, the coherence/backscatter statistics are obtained on polygons for each combination of forest type and topographic condition (area > 1.5 ha), allowing to examine the coherence/backscatter behavior versus forest type, topography or biomass for homogeneous units.

General coherence behavior

Figure 2 presents a color composite of 3 tandem image processed with GAMMA software: July (red), August (green) and March (blue). The dark color (dark red and purple) indicates strong coherence change between the different tandem, which will be studied further in this section. Globally, brighter areas with yellow tones correspond to grasslands, mainly on the western part of the image, which exhibit the highest correlation. Forested areas appear in green with darker tones, as well as the mountainous area at the right bottom of the image. Figure 3 presents mean correlation values, calculated with DIAPASON, for 4 land-use types, plotted against time interval. The best coherence and discrimination between themes is obtained for the tandem data, and the coherence decreases with time interval for all themes. However, after a given time interval, the coherence does not vary anymore. For the lower time intervals it is possible to discriminate deciduous from coniferous, indicating that tandem data or low time interval interferograms offers possibilities for general land-use discrimination, which was not possible using ERS backscatter intensity alone.

Figure 4 shows the coherence measurements for four different themes, deciduous, coniferous, sparse forest and grasslands for the two tandem summer acquisitions processed with GAMMA. It appears (Table 2) that deciduous are the less coherent (< 0.3), coniferous show intermediate values (0.3-0.5) and grasslands and sparse themes are the more coherent (> 0.5). The coherence values for a given theme show an important dispersion leading to overlapping between themes. A temporal variability of the grassland signatures between the two summer acquisitions although the meteorological conditions were very closed is observed. It is probably related to different ground conditions corresponding for grass to different growing stage. The rough theme definition in the inventory, which does not indicate the various growth stages for each species, explains the large range of values for a given theme. Moreover a part of the variability should be attributed to errors in the inventory dating from 5 years before the tandem acquisitions.

These observations can be interpreted as follows: as introduced in the first section the loss of coherence must be mainly attributed to geometric and dielectric change of the targets between each interferometric acquisition, $\rho_{temporal}$ in (2). As mentioned in previous studies (Floury et al., 1996), the decrease of the coherence with volume scattering can be explained by: 1) a diminishing ground contribution, which is generally geometrically and dielectricly stable thus highly coherent; 2) an increasing volume contribution, which is less coherent, due to targets motions (mainly leaves or needles at C-band) under the wind between the acquisitions. This explains the coherence decrease as the foliar biomass increase from grasslands/young forests to mature forests. However this general behavior previously observed in other papers must be studied as a function of environmental factors. In particular, geometric and dielectric change must be addressed for a wide field of applications.

Meteorology

Figure 5 shows the coherence measurements using the same themes in Figure 4 but for a summer (July) and a winter (February) acquisition. It appears clearly that the behavior of certain themes is strongly affected by both seasonal and local weather conditions leading to strong variability of the coherence signatures. It is well traduced by the statistics presented in the Table 2 for the average coherence values of the different vegetation categories as a function of dates. Except for deciduous, the results show an increase of the average coherence values from February to August. In the deciduous case ,the higher winter coherence values should be attributed to the leaf-off trees, leading to an increased soil contribution, highly coherent. In February the area was entirely snow covered. The strong dispersion of the winter coherence values of grasslands is probably due to these snow conditions which affect the coherence depending on its nature. Indeed, wet snow usually leads to low coherence values due to scattering geometry changes (i.e. freezing/thawing cycles) while shallow dry snow shows coherence generally similar to the snow free case. The low coniferous coherence in the February acquisitions is probably due to the same reason. These effects, if they are homogeneous over a whole region, can represent an advantage for discriminating between different themes. As expected, the deciduous themes exhibit higher coherence when they are leaf-off.

Topography

The dispersion observed in the summer acquisitions, even for low-vegetalized themes (Figure 4) cannot be attributed to meteorological effects (no rain, low wind conditions). Looking to the coherence color composite (Figure 2) it appears that mountainous areas exhibit low coherence showing the coherence is affected by the local topography. Figure 6 shows coherence versus the local aspect angle for increasing slopes classes and for grasslands areas all over the image for which coherence should be stable and high in summer conditions. An aspect angle of 90° degrees corresponds to a terrain surface normal towards the satellite. For this aspect angle the strongest slope dependence of the coherence estimate is observed. The explanation of this dependence is the geometric decorrelation (i.e. the higher baseline decorrelation effect) caused by the non-overlapping fraction of the range spectral band, as the band filters were calculated for the case of a horizontal surface, which is too wide for the slopes facing the SAR (Gatelli et al., 1994).

For slopes away from the SAR, i.e. aspect angles around 270°, the band filters are narrower than necessary, but no decorrelation is caused. However, reduced coherence on slopes facing away from the sensor as a function of the slope is also observed. The explanation of that is the different weighting of the backscattering between soil and vegetation. The incidence angle dependence of the soil is much stronger than that of the vegetation. Therefore, the relative contribution of the stable soil to the total backscattering decreases with increasing incidence angle.

Regarding a possible correction of the coherence vs. slope angle, one should say that the geometric decorrelation for the mountain face which is tilted toward the satellite could be compensated by using the information of the DEM during the computation of the interferogram (i.e. when common band filtering is applied) but this is time consuming and is not implemented in the GAMMA and DIAPASON softwares. On the other hand, the decrease of the coherence for the mountain face that is tilted away from the sensor is a physical consequence of the imaging geometry (incidence angle dependence of the backscattering coefficient) and in our opinion is not to be corrected. That way, without correction, only gently rolling terrain and areas without layover should be readily used for interpretation. In the following we will arbitrary reject areas with slopes superior to 15° in order to reduce confusion.

3.1.2 Classification results using the tandems

Results point out the sensitivity of coherence data to biophysical parameters but also the necessity to take into account topographic and meteorological factors for an interpretation of land-use interferometric signatures. Using these observations, we study forest mapping using classification methods applied on the tandem images.

Method

We use in the following the supervised maximum likelihood algorithm, which is based on the assumption that data are normally distributed. Although this is not the case for SAR data, we verified that processed data are closed to a Gaussian distribution thanks to the high multi-look achieved. Class statistics are obtained on training polygons (1% of the total area to be classified) derived from the digital inventory covering 50 by 80 km, and the validation through confusion matrices is made on a second set of independent polygons (> 50 % of the area to be classified). Three data sets are used. The first approach uses one tandem pair, the second approach two tandem pairs and the third approach four tandem pairs plus backscatter ratios between dates.

Forest/ non Forest

With one tandem pair, the only reliable classification is forest/non-forest. The forest/non-forest separation is possible provided that forested areas present always the lowest values in coherence (Figure 3), due to temporal decorrelation. Figure 7 represents the forest inventory and Figure 8 displays the classified image while confusion matrix is shows in Table 3. Masked areas in Figure 8 (black) include non-vegetation themes (urban, water and slopes larger than 15°, including layover areas). All the non-forested themes (shrubs, grasslands) in the forest inventory are defined as non-forest. The overall accuracy is 94 %, which is satisfactory for application purposes. It is noticeable that adding the backscatter intensities to the coherence improve the results by only 5 %. The best results are obtained using the summer tandems in which no meteorological effects (snow, freezing) are observed. Using the winter tandems the results are lower (of about 80 % global accuracy) mainly because the meteorological effects described in section 3.1.1 are not homogeneous on the whole image. That way, forest/non-forest classification shows very satisfactory results using appropriate data, showing that interferometry is an interesting tool for change detection caused by fires or forest management.

Multi species/biomass categories discrimination

With two tandem pairs, a four-class classification is feasible, splitting the forest category into two parts: roughly a high foliar biomass (mature coniferous and deciduous stands) and a low foliar biomass class (sparse and young coniferous). An urban area class can be discriminated, providing that built-up areas have characteristic signatures: both high coherence and high backscatter level. The confusion matrix (Table 4) shows lower accuracy results with an overall accuracy of 75 %, which is lower compared to the one tandem classification case. This lower result can be attributed to the defined typology in the forest inventory which not suitable with the one achievable by radar data, based on a phenomenological basis. Some classes defined in the inventory, as sparse coniferous or reforested areas are not sufficiently accurate to determine in which biomass range they should appear.

As certain themes exhibit typical seasonal behavior regarding the coherence and the intensity, a more detailed classification can be made based on the above observations: deciduous / spruce / others mature coniferous / young coniferous / young Austrian pine / shrublands / grasslands / urban areas / water. This last classification was made using the four ERS tandem pairs, plus 4 backscatter changes related to the August scene (total of 16 independent channels). The overall accuracy is of 72 %, the coniferous themes such as spruce being the best classified with an accuracy of 76.7 % (Table 5). The lowest accuracy is for the deciduous theme (63 %), which is mainly due to overlapping with coniferous, caused by variable stand age or density. Some themes present a strong seasonal backscatter variability (e.g. the low vegetalized themes) as mentioned in section 3.1.1. Otherwise spruce and coniferous present very stable signatures. Consequently the use of backscatter ratio is very useful, in particular the ratio between summer and winter acquisitions, improves the results by 20%.

The global accuracy achieved in the two latter classifications indicates that coherence images should be useful to realize pre-inventories in order to determine rough biomass/vegetation types classes. However the coherence sensitivity to environmental factors such as meteorology and topography, shows that they must be take into account for a global classification strategy. Particularly, attention must be paid to meteorological effects on coherence and backscatter according to the themes you are trying to discriminate. It appears that contrasted conditions are useful for multi species/biomass classes discrimination, even without knowledge of the meteorological conditions. Finally, the strongest limitation is the topography, which highly affects the general behavior of coherence. Without any correction, we propose to remove these areas by using slope criteria over which coherence should not be used for interpretation purpose.

3.2 Retrieval forest biomass

3.2.1 Degree of coherence sensitivity to forest biomass

After having studied the general behavior of the coherence and how it is affected by environmental factors, we now focus on single specie, the Austrian black pine, to investigate more in detail the link between coherence and biophysical parameters. In particular coherence sensitivity to conventional forest parameters such as height and stem biomass is assessed.

General coherence behavior

Figure 9 presents the coherence estimated for various ERS pair acquisition as a function of stem biomass. Full lines are those obtained from linear regression while accuracy is given by the dashed lines which indicates the 95% confidence interval corresponding approximately to ± 3 standard deviations given by (Hagberg et al., 1995):

$$\sigma_\rho = \frac{1-\rho^2}{\sqrt{2N}} \qquad (3)$$

where zero-mean Gaussian white noise process is assumed and N is the number of independent samples. N must be large in order to get an improved precision, especially for areas where the degree of coherence is low. This is why, two types of confidence limits are obtained as a function of stem volume. Indeed, up to 108 tons/ha stem biomass, the statistics are calculated by using around 120 independent samples while up to 300 independent samples are used beyond.

As shown in Figure 9, a coherence decrease with stem biomass is observed. Herland (1995) and Smith et al. (1998) observed such tendency for boreal forest stands indicating higher correlation values for young forests compared to mature forests. The linear correlation could be interpreted in the way presented in section 3.1.1. At C-band, forest backscatter mainly originate from twigs and needles (volume scattering) in addition to direct ground scattering which contributes more or less with soil moisture and roughness along with transmissivity and forest fraction cover which in turn is linked with growth stage. Higher correlation for young pines compared to mature ones can be explained by higher ground contribution and/or higher trees stiffness. Then, correlation decrease with stem biomass is mainly due to ground contribution decreases with the growing contribution of scatterers more sensitive to temporal variations. Except for both winter tandem pair cp02&cp03 and for cp4-7 spring fall pair, significant linear correlations (at $p = 0.001$ or better) are found between coherence and the forest parameters. Higher regression slopes are observed for the cp08 and cp07 tandem pairs while lower regression slopes values are with the spring-fall cp4-7 pair that have high baseline and interval day acquisition, and with the cp02 winter tandem image. On other hand, cp08 DIAPASON and GAMMA pairs have approximately the same behavior absolute level dependent as indicated before at section 2.2. Furthermore, no coherence saturation clearly appears with increasing stem volume. Table 6 synthesizes the statistic parameters for all interferometric pairs and main forest parameters investigated. As expected, higher values of R^2 from 0.36 to 0.55 ($p>0.001$) as well as regression slopes are obtained for summer tandem pairs cp08 and cp07 compared to both winter pairs affected by meteorological effects (see section 3). Note that same results are also obtained between both cp08 pairs. Otherwise, other pairs give intermediate results, which depend on day interval between acquisitions and meteorological conditions. Finally these results indicate that the tandem data are the best sensitive to conventional forest parameters. In order to use coherence data in a forest biomass retrieval scheme, accurate interpretation is needed. Especially to determine explanation of best negative linear correlation (R^2 = 0.55) associated with worst coherence accuracy (higher RMSE values up to 0.12). Indeed, same stem volume – around 144 tons/ha for example – shows a coherence dynamic range up to 0.35.

Meteorology

In order to investigated furthermore these general behaviors, temporal decorrelation due to volume scattering at C-band should be considered at 2 different time spans. First, on a monthly basis during the growing season, the crown geometry changes due to annual new shoots (about 30 cm), which is probably a source of significant decorrelation. Second, on a very short time basis (maybe down to few seconds), decorrelation occurs due to random motions of the scatterers (needles and twigs) under the wind influence. In this last case, it should depend on the local wind speed over the canopy, in addition to the topographic exposure to wind that will be described in the following.

For ERS configuration, little displacements are enough to decorrelate the signal (Zebker and Villasenor, 1992), even for weak winds. In our case, we consider that the topography attenuates the speed of the wind giving a local wind vector $\mathbf{W_{loc}}$ depending on a wind exposure angle called θ_w angle between the wind vector $\mathbf{W}$ and the normal vector to the terrain $\mathbf{n}$ defined as (Beaudoin et al., 1996):

$$\theta_w = \cos^{-1}\left[\sin\alpha \cdot \cos(\beta - \beta_w)\right] \tag{4}$$

with α and β being the terrain slope and aspect angles, and β_w the wind direction. A value of 0° concerns a vertical slope opposite to the wind direction while values of 90° and 180° are respectively for a flat terrain ($\alpha = 0°$) and for a vertical slope facing the wind direction.

As it was shown in the section 3.1.1, the topography affects strongly the coherence in the highest slope areas. Consequently we will work with stands over weak slopes i.e. lower than 15°. Figure 10 considers two data subsets corresponding to young and mature pines, in which coherence values of the cp08 DIAPASON tandem pair are plotted against the wind exposure angle (θ_W). A weak wind (~10 km/h) was measured at this date. Results show that, for young pines (0-108 tons/ha, Figure 10a) no relationship with θ_W is observed, probably due to the correlation mainly driven by the ground contribution, in addition to the higher stability of young trees under the local wind influence. Therefore, dispersion in Figure 10a could be explained in the variability of the transmissivity and the cover fraction, in addition to soil moisture and roughness that all modulate the ground contribution. On the other hand, for mature trees (108-216 tons/ha, Figure 10b), the coherence is highly correlated to θ_W, with a quasi-linear decrease ($R^2 = 0.78$), which partially explains the high dispersion around the trend indicating that a weak wind easily deccorelates the signal. To go further, a dynamic model that relates the vegetation element motions to local wind speed is needed. Unfortunately, such model does not exist at the time, and the link between the displacement of vegetation elements and the wind and forest parameters has been merely investigated experimentally. Only trunk movements under wind have been studied for wind damage prevention in forests (Gardiner, 1995).

Results show the sensitivity of coherence data to forest parameters and also point out the necessity to take into account topographic and meteorological conditions. We now use in the following the best tandem data (i.e. cp08 and cp07 pairs) to retrieve forest parameters.

3.2.2 Forest biomass retrieval results using tandems

Method

The method is based on the simple straight-line model describe by the statistic parameters (see Table 7). We have calculated the accuracy (RMSE) of the forest parameter retrieval possible using the different correlation images. In this case, we consider two data subsets defined randomly corresponding respectively to the data used for fitting the line (training data) and for inversion (control data). Hence, accuracy derived using this cross validation method give us an expected range for retrieval such forest parameters. Three data sets will be used. The first approach uses all stands, the second approach stands with weak slopes and the third approach stands with weak slopes plus wind effect empirically normalize for high stem biomass stands.

For all stands

Table 7a synthesizes the parameters of the linear models used for inversion as well as the results of forest parameters retrieval. Note that in this case 55 stands are used, as training data while 48 are control data. The results are approximately identical for all the pair and forest parameters. Hence RMSE are centered for height and stem biomass respectively around 6.7 m and 57 tons/ha. Accuracy retrieval seems to be independent with the forest parameter range, probably due to the no saturation observed in the coherence data. Finally, looking at cp08 pair results it also appears variations possibly explained by different processing techniques as noted above. Obviously, the accuracy level remains quite low for retrieve forest biomass over hilly terrain. As indicated before one possible cause of errors could be attributed to topography. To this aim, same approach is used for the stands located on weak slopes.

For stands with weak slope (<15°)

A summary of the results is given in Table 7b. Note that in this case only 92 stands are used leading to 50 stands for training and 42 stands for control. 9 of the 11 stands not used correspond to high stem volume stands. First it appears that inversion results are systematically improved whatever tandem pair and forest parameters. That way best results for height and stem biomass are respectively 6 m and 48 tons/ha. These results are closely correlated with steeper fitted line – corresponding to higher regression slopes (a) – indicating a greater sensitivity for forest parameters. Otherwise results exhibit some accuracy differences probably due to the processing technique. Nevertheless, results are no enough sufficient towards an operational biomass retrieval scheme using coherence data. This could be due to the wind, which has been pointed before as a source of error (Figure 10b). In the next part, the cp08 coherence is corrected taking into account the local wind exposure angle θ_w using the equation showed in Figure 10b. The correction is applied on 31 high stem volume stands.

For stands with weak slope (<15°)/wind effect normalize

Results (Table 8) indicate a slight increase of the accuracy level round, 0.2 m and 2 tons/ha respectively for height and stem biomass. Consequently, these results indicating that wind effect correction have a poor impact on the improvement of inversion accuracy. One explanation could be that the dynamic range of retrieval accuracy is mainly determined by that of the low stem biomass which still exhibit higher dispersion.

The results shown here are better than those obtained by using ERS intensity alone, which systematically show the worst estimation results. The coherence results can be compared to that of multi-polarimetric L band SIR-C data, well known to give better estimations than ERS, concerning biomass retrieval. Harrel et al. (1997) obtained on a pine forest with a similar range of stem volume (< 200 tons/ha) estimation errors from 59 to 86 tons/ha. Finally, improvement in the biomass estimation with ERS as well as with others SAR configurations is expected by combining intensity and ERS coherence data.

The global accuracy achieved indicates that coherence measurements can be usefully employed for forest parameters retrieval over forests located in weak slope areas (< 15°) at large scale. However, the high dynamic range of coherence observed on low stem biomass in relation with topography and environmental conditions must be assessed furthermore towards the development of an operational biomass retrieval scheme.

4 Concluding remarks

In this paper, ERS DEM-differential interferometric correlation was investigated over a hilly-forested test-site. The degree of coherence was found to be a good land-use discriminator for major land-use types and forest biomass estimator especially using short time intervals. It was shown in particular that efficient forest/non-forest classifications (accuracy > 90%) are feasible using only one summer tandem pair. More detailed classification, with discrimination between forest themes, have been done showing that multi-temporal data using coherence plus backscatter and backscatter ratio is very interesting. On forest covers, the correlation is linked to conventional forest parameters such as stem volume (R^2 = 0.55) – correlated with the growth stage –, due to decreased ground contribution and increased crown volume scattering, originating mainly from needles and twigs. Furthermore the results do not indicate that coherence saturates for volumes up to 250 tons/ha allowing the use of the simple straight-line relationship between coherence and forest parameters for a retrieval scheme. With the more stable meteorological conditions, global accuracy of the retrieval appears to be 5.8 m and 46 tons/ha for respectively height and stem biomass.

However, the study points out some problems related to topographic and environmental conditions, which needed to be take into account. First, strong slopes areas (> 15°) were not involved in the classification and biomass retrieval scheme because of the unreliable coherence values encountered. Further improvement for taking into account of this effect in the interferometric processing chain is needed. Second, it appears that even with one-day interval acquisition, attention must be paid to meteorological conditions. In particular for ERS configuration a rapid decorrelation is easily generated by weak winds (10 km/h). Hence, the correlation behavior with the wind speed was highlighted using the tandem scene, through the variation of the local wind speed due to the topographic exposure to wind. Following these observations it seems that for biomass retrieval applications the user should select images for which he knows the meteorological conditions were stable (low wind, no snow coverage). On the contrary, and for multi-species classification purpose, selecting images with strong contrast improves classification result, using the backscatter change information along with the degree of coherence.

The work presented in this paper is included in an inductive approach based on statistical results. A difficult task is to use directly the results for generalization purpose to other site, however the results presented here contribute as a new step towards generalization purpose of such tools. Indeed, the specificity of the test site help us to point out what are specific effects of interferometric, topographic and environmental conditions on the use of INSAR data for forest monitoring. It brings also experimental results on the identification impact of such previous conditions on the coherence variability and consequently on the estimation of forest attributes.

Therefore, for generalization purposes, the challenge will be to determine how the degree of coherence can be linked robustly to characteristics of interest. Carrying on such work is probably worthwhile, considering the potential of interferometric SAR data in addition to the usual backscatter information.

Acknowledgments

This work was performed within a joint LCT-SCOT project funded by the CNES (contract # CNES/94/0239) and the European project EUFORA, that we would like to warmly thank. Particularly, we thank Thierry Rabaute and Didier Massonnet for the access to the CNES interferometric processor. Thanks also go to ESA for providing the SAR data within the project-pilot PP2-F132, and P. Gigord from IGN who provided us with the DEM (BD CARTO IGN ©) within collaboration on the correction of SAR bacskcatter data acquired over hilly terrain. T. Castel was supported by a grant from Ademe and Cemagref. Finally, the authors gratefully acknowledge the useful comments, corrections and suggestions made by the peer reviewer of this paper.

References

Askne, J. I. H., Dammert, P. G. B., Ulander, L. M. H., and Smith, G. (1997), C-band repeat-pass interferometric SAR observations of the forest. *I.E.E.E. Transactions on Geoscience and Remote Sensing*, 35:25-35.

Beaudoin, A., Castel, T., Deshayes, M., Stussi, N., Stach, N., and Le Toan, T. (1995), Biomass retrieval over hilly terrain from spaceborne SAR data. *First international workshop on "Retrieval of bio and geophysical parameters from SAR data for land applications"*, Toulouse, France, 10-13 October, 131-141.

Beaudoin, A., Castel, T., and Rabaute, T. (1996), Forest monitoring over hilly terrain using ERS INSAR data. *Fringe '96 Workshop*, Zurich, Switzerland.

Beaudoin, A., Le Toan, T., Goze, S., Nezry, E., Lopes, A., Mougin, E., Hsu, C. C., Han, H. C., Kong, J. A., and Shin, R. T. (1994), Retrieval of forest biomass from SAR data. *International Journal of Remote Sensing*, 15:2777-2796.

Castel, T. (1998), Estimation de paramètres de la ressource forestière par télédétection radar à synthèse d'ouverture. Apport du couplage d'un modèle architectural de plantes avec un modèle de diffusion électromagnétique. Ph. D. Thesis, ENGREF, Montpellier France, 250 p.

Dobson, M. C., Pierce, L., Sarabandi, K., Ulaby, F. T., and Sharik, T. (1992), Preliminary analysis of ERS-1 SAR for forest ecosystem studies. *I.E.E.E. Transactions on Geoscience and Remote Sensing*, 30:203-211.

Dobson, M. C., Ulaby, F. T., Pierce, L. E., Sharik, T. L., Bergen, K., Kellndorfer, M., Kendra, J. R., Li, E., Lin, Y. C., Nashashibi, A., Sarabandi, K., and Siqueira, P. (1995), Estimation of forest biophysical characteristics in northern Michigan with SIR-C/X-SAR. *I.E.E.E. Transactions on Geoscience and Remote Sensing*, 33:877-895.

Floury, N., Le Toan, T., and Souyris, J. C. (1996), Relating forest parameters to interferometric data. *Proceedings of IGARSS'96 Symposium*, Lincoln Nebraska USA.

Floury, N., Le Toan, T., Souyris, J. C., and Bruniquel, J. (1997), A study of SAR interferometry over forests: theory and experiment. *Proceedings of IGARSS'97 Symposium*, Singapore, 1868-1870.

Gardiner, B. A. (1995), The interaction of wind and tree movement in forest canopies. Wind and trees (M. P. Coutts & C. J. Grace, Ed), Cambridge University Press, Cambridge.

Gatelli, F., Monti Guarnieri, A., Parizzi, F., Pasquali, P., Prati, C., and Rocca, F. (1994), The wavenumber shift in SAR interferometry. *I.E.E.E. Transactions on Geoscience and Remote Sensing*, 32:855-865.

Gens, R., and van Genderen, J. L. (1996), Review article : SAR interferometry--issues, techniques, applications. *International Journal of Remote Sensing*, 17:1803-1835.

Hagberg, J. O., Ulander, L. M. H., and Askne, J. (1995), Repeat-pass SAR interferometry over forested terrain. *I.E.E.E. Transactions on Geoscience and Remote Sensing*, 33:331-340.

Harrell, P. A., Kasischke, E. S., Bourgeau-Chavez, L. L., Haney, E. M. and Christensen Jr. N. L., (1997), Evaluation of approaches to estimating aboveground biomass in southern pine forests using SIR-C data, *Remote Sensing Environment*, 59:223-233.

Herland, E. A. (1995), SAR interferometry with ERS-1 in forested areas. *Proceedings of IGARSS'95 Symposium*, Florence Italy, 202-204.

Kasischke, E. S., Bourgeau-chavez, L. L., Christensen, J., N. L., and Haney, E. (1994), Observations on the sensitivity of ERS-1 SAR image intensity to changes in aboveground biomass in young loblolly pine forests. *International Journal of Remote Sensing*, 15:3-16.

Massonnet, D. (1994), Validation of ERS-1 interferometry at CNES. *Second ERS-1 Symposium*, Hamburg Germany, 703-709.

Massonnet, D., and Rabaute, T. (1993), Radar interferometry : limits and potential. *I.E.E.E. Transactions on Geoscience and Remote Sensing*, 31:455-464.

Ranson, K. J., Saatchi, S., and Sun, G. (1995), Boreal forest ecosystem characterization with SIR-C/X-SAR. *I.E.E.E. Transactions on Geoscience and Remote Sensing*, 33:867-876.

Smith, G., Dammert, P. G. B., Santoro, M., Fransson, J. E. S., Wegmüller, U., and Askne, J. I. H. (1998), Biomass retrieval in Boreal forest using ERS and JERS SAR. *Second International Workshop on "Retrieval of Bio- and Geo-physical Parameters from SAR data for Land Applications"*, Noordwijk, The Netherlands, 21-23 October, in press.

Strozzi, T., Dammert, P., Wegmüller, U., Martinez, J.-M., Beaudoin, A., Askne, J., and Hallikainen, M. (1998), European forest mapping with SAR interferometry. *Second international workshop on "Retrieval of Bio- and Geo-physical Parameters from SAR data for Land Applications"*, Noodwijk, The Netherlands, 21-23 October, in press.

Ulander, L., Dammert, P. B. G., and Hagberg, J. O. (1995), Measuring tree height with ERS-1 SAR interferometry. *Proceedings of IGARSS'95 Symposium*, Florence Italy, 2189-2191.

Wang, Y., Kasischke, E. S., Melack, J. M., Davis, F. W., and Christensen Jr, N. L. (1994), The effects of changes in loblolly pine biomass and soil moisture on ERS-1 SAR backscatter. *Remote Sensing Environment.*, 49:25-31.

Wegmüller, U., and Werner, C. (1995a), SAR interferometric signatures of forest. *I.E.E.E. Transactions on Geoscience and Remote Sensing*, 33:1153-1161.

Wegmüller, U., and Werner, C. L. (1995b), Farmland monitoring with SAR interferometry. *Proceedings IGARSS'95 Symposium*, Florence Italy, 544-546.

Wegmüller, U., and Werner, C. L. (1997), Retrieval of vegetation parameters with SAR interferometry. *I.E.E.E. Transactions on Geoscience and Remote Sensing*, 35:18-24.

Wegmüller, U., Werner, C. L., and Strozzi, T. (1998), SAR interferometric and differential interferometric processing chain. *Proceedings IGARSS'98 Symposium*, Seattle Washington USA, 1106-1108.

Zebker, H. A., and Villasenor, J. (1992), Decorrelation in interferometric radar echoes. *I.E.E.E. Transactions on Geoscience and Remote Sensing*, 30:950-959.

Table 1. Summarize of all the interferometric acquisitions used for interpretation in this paper.

ERS Pairs	**Baseline** (m)	**Processing chain**	**Acquisition Time**			**Wind speed**		**Air Temp.**	
			Date	Day interval	Season	Date 1 (m/s)	Date 2 (m/s)	Date 1 (C°)	Date 2 (C°)
cp2-3	126	Diapason	25/08/92 28/01/93	210	Summer Winter	3.5	8	26.4	2.9
cp2-5	124	Diapason	25/08/92 17/06/93	296	Summer Summer	3.5	5	26.4	18.3
cp3-5	65	Diapason	28/01/93 17/06/93	140	Winter Summer	8	5	2.9	18.3
cp4-7	133	Diapason	08/04/93 04/11/93	156	Spring Fall	4	5	13.1	11.3
cp07 Tandem	44	Gamma	15/07/951 06/07/95	1	Summer	5	4	22	24
cp08 Tandem	98	Diapason & Gamma	19/08/95 20/08/95	1	Summer	4	3	28	25
cp02 Tandem	71	Gamma	17/02/96 18/02/96	1	Winter	2	3	1.2	0.1
cp03 Tandem	20	Gamma	12/03/96 13/03/96	1	Spring	3	2	0	1.7

Table 2. Confusion matrix for the forest/non forest classification with one tandem pair, overall accuracy is 94 %.

Classified / Reference	Forest	Non-forest
Forest	**96 %**	9 %
Non-forest	4 %	**91 %**

Table 3. Confusion matrix for the classification using two tandem pairs, overall accuracy is 75%.

Classified / Reference	High biomass	Low biomass	Non-forest	Water	Urban areas
High biomass	**72 %**	19.6 %	2.6 %	0.5 %	9 %
Low biomass	18.6 %	**62 %**	10.9 %	0.3 %	5.75 %
Non-forest	6.5 %	18.6 %	**81 %**	0.1 %	18.3 %
Water	0 %	0 %	0 %	**99.1 %**	0 %
Urban areas	2.7 %	0 %	5.6 %	0 %	**67 %**

Table 4. Confusion matrix with four tandem pair plus backscatter ratio, overall accuracy is 72%.

Classified / Reference	Deciduous	Spruce	Dense Coniferous	Med. Coniferous	Young Austrian Pine	Sparse	Grasslands	Urban areas	Water
Deciduous	**63.35**	4.97	9.76	0.99	0.00	1.75	0.40	0.20	0.00
Spruce	3.81	**76.68**	4.45	15.44	0.00	2.73	0.00	0.10	0.00
Dense Coniferous	24.38	3.76	**72.61**	1.77	12.01	5.81	7.08	2.58	0.00
Med. Coniferous	0.13	14.17	1.09	**62.56**	0.00	5.09	0.03	0.00	0.00
Young Austrian. Pine	0.02	0.00	1.40	0.06	**57.31**	0.37	2.46	1.01	0.00
Sparse	6.62	0.00	9.43	19.16	7.78	**80.85**	14.04	6.12	0.06
Grasslands	0.06	0.00	0.08	0.00	22.91	1.78	**73.15**	5.31	0.00
Urban areas	0.48	0.00	0.02	0.02	0.00	0.19	0.78	**84.67**	0.00
Water	0.01	0.42	0.00	0.00	0.00	0.01	0.02	0.00	**99.94**

Table 5. Synthesis of statistics calculated from ERS coherence images of the *Lozère* test site. R^2 is the correlation coefficient, a is the slope of the linear regression, b is the intercept of the regression line with the Y-axis and RMSE is the root mean square error given by $\mathrm{RMSE} = \left[\sum (y - \hat{y})^2 / N \right]^{1/2}$ and $y = a\hat{y} + b$.

ERS pairs	Age (years)				Height (m)				Stem volume (m^3/ha)			
	RMSE of ρ	R^2	a ($\times 10^{-3}$)	b	RMSE of ρ	R^2	a ($\times 10^{-3}$)	b	RMSE of ρ	R^2	a ($\times 10^{-3}$)	b
DIAPASON												
cp08	0.11	**0.51**	-3.45	0.75	0.12	**0.37**	-12.9	0.76	0.11	**0.46**	-0.5	0.72
cp4-7	0.09	0.07	-0.76	0.40	0.09	0.07	-3.55	0.41	0.09	0.07	-0.13	0.40
cp3-5	0.11	0.31	-2.36	0.63	0.11	0.35	-11.2	0.67	0.11	0.31	-0.37	0.32
cp2-3	0.10	0.18	-1.43	0.46	0.09	0.20	-6.56	0.48	0.10	0.16	-0.21	0.45
cp2-5	0.09	0.18	-1.32	0.44	0.09	0.19	-5.92	0.46	0.09	0.18	-0.2	0.43
GAMMA												
cp07	0.11	**0.53**	-3.83	0.52	0.11	**0.52**	-16.8	0.56	0.11	**0.55**	-0.61	0.50
cp08	0.09	**0.51**	-3.03	0.51	0.11	**0.36**	-11.2	0.51	0.10	**0.49**	-0.46	0.49
cp02	0.05	0.14	-0.64	0.17	0.05	0.03	-1.36	0.16	0.05	0.13	-0.09	0.16
cp03	0.04	0.00	0.002	0.10	0.03	0.02	0.62	0.10	0.04	0.00	-0.002	0.11

Table 6a. Retrieval statistics calculated from tandem ERS coherence images of stands located on *Lozère* test site. The legend is the same as table 5.

ERS pairs	Age (years)				Height (m)				Stem volume (m^3/ha)			
	a	b	R^2	RMSE	a	b	R^2	RMSE	a	b	R^2	RMSE
cp08 DIAPASON	-155	139	0.62	**25.5**	-35.1	34	0.56	**6.7**	-1068	897.6	0.61	**172**
cp 07	-133.6	95.6	0.61	**27**	-32.6	25.1	0.60	**6.3**	-922	600.4	0.63	**158**
cp 08 GAMMA	-181.7	116	0.64	**29.5**	-40.8	28.7	0.61	**7.7**	-1231	732.7	0.56	**186**

Table 6b: Statistics calculated from tandem ERS coherence images for the stands located on weak slopes (< 15°) of the *Lozère* test site. The legend is the same as table 5.

ERS pairs	Age (years)				Height (m)				Stem volume (m^3/ha)			
	a	b	R^2	RMSE	a	b	R^2	RMSE	a	b	R^2	RMSE
cp08 DIAPASON	-160	141.2	0.63	**22**	-37	35	0.59	**6.2**	-1067	889	0.61	**133**
cp 07	-133	95.2	0.58	**25**	-32.9	25.1	0.62	**5.8**	-891	583.5	0.56	**136**
cp 08 GAMMA	-202	123.7	0.68	**25**	-44.5	30.1	0.57	**6.9**	-1294	752.6	0.60	**153**

Table 7. Retrieval statistics calculated from cp08 DIAPASON tandem ERS coherence images for the stands located on weak slopes (< 15°) and wind effect normalize for high stem volume stands. The legend is the same as table 5.

Forest parameters	cp08 DIAPASON interferometric pair			
	a	b	R^2	RMSE
Age (years)	-173	148	0.70	**21**
Height (m)	-39.8	36.5	0.64	**6**
Stem volume (m^3/ha)	-1130	923.5	0.65	**129**

List of figures

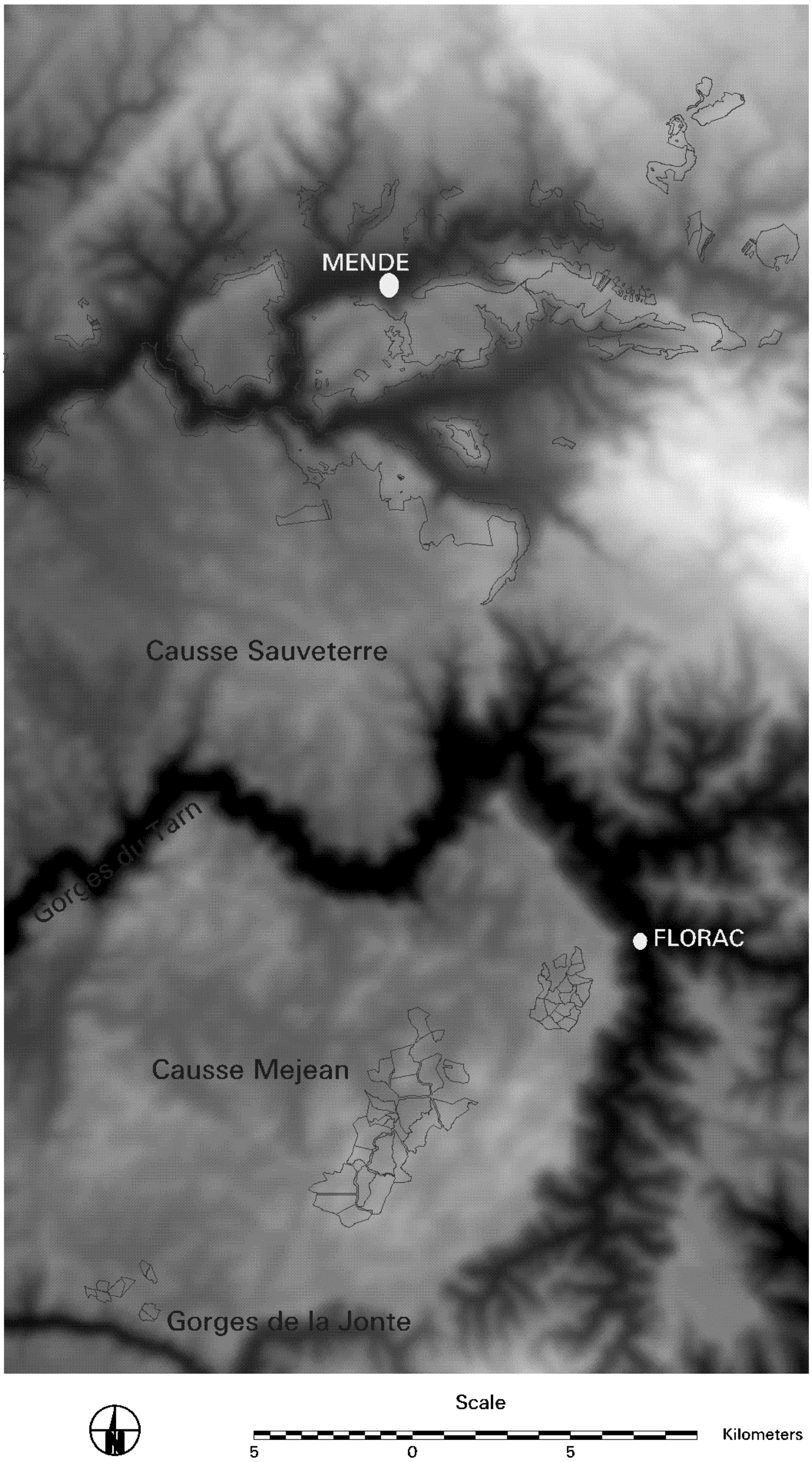

Figure 1: DEM and forest limits (Austrian black pine plantations, gray lines) over the test-site.

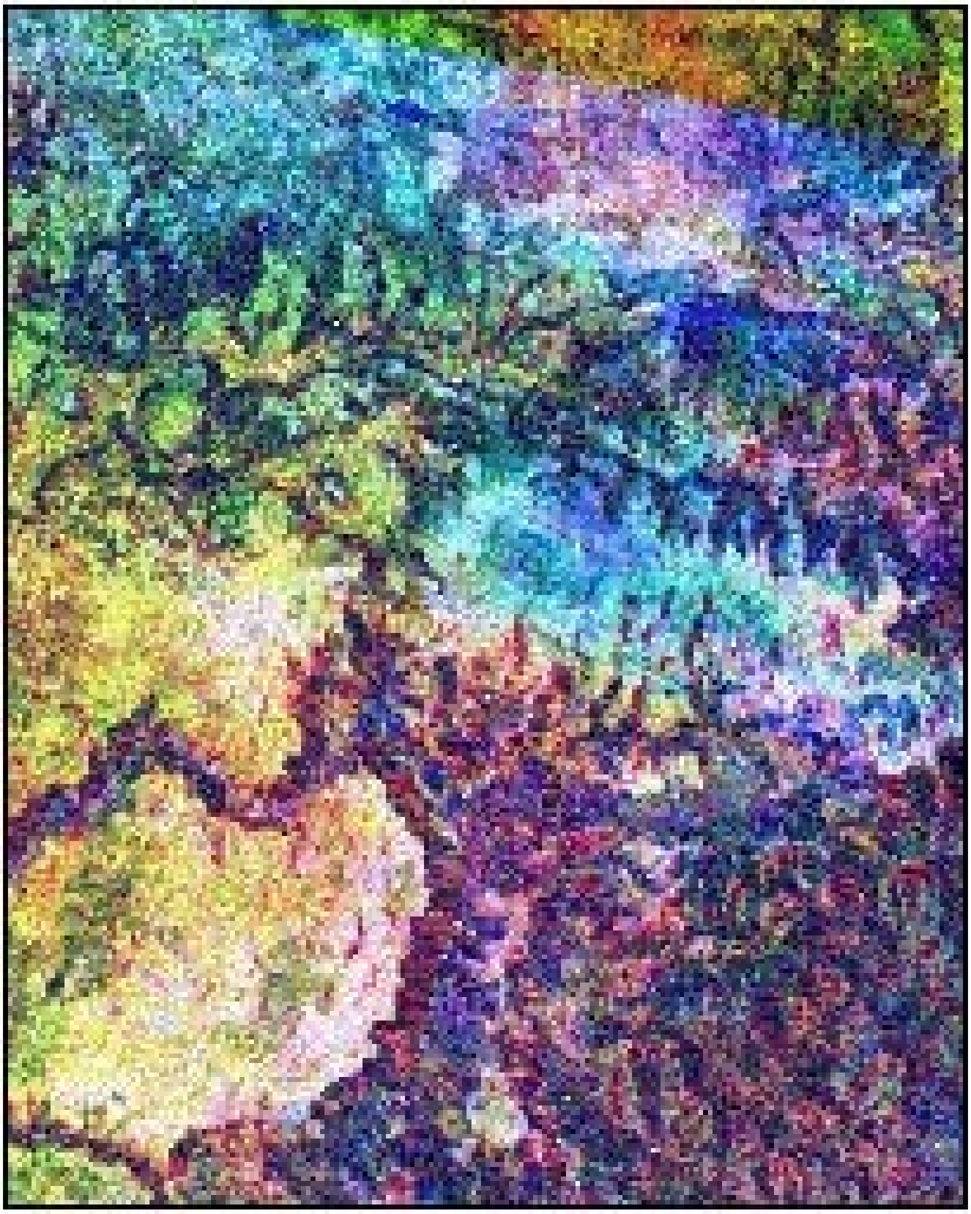

Figure 2: False colors composite of the coherence extracted from July (cp07: Red), August (cp08: Green) and February (cp02: Blue) acquisitions. Grasslands and bushlands appear as white or light tones, the darker tones being forest.

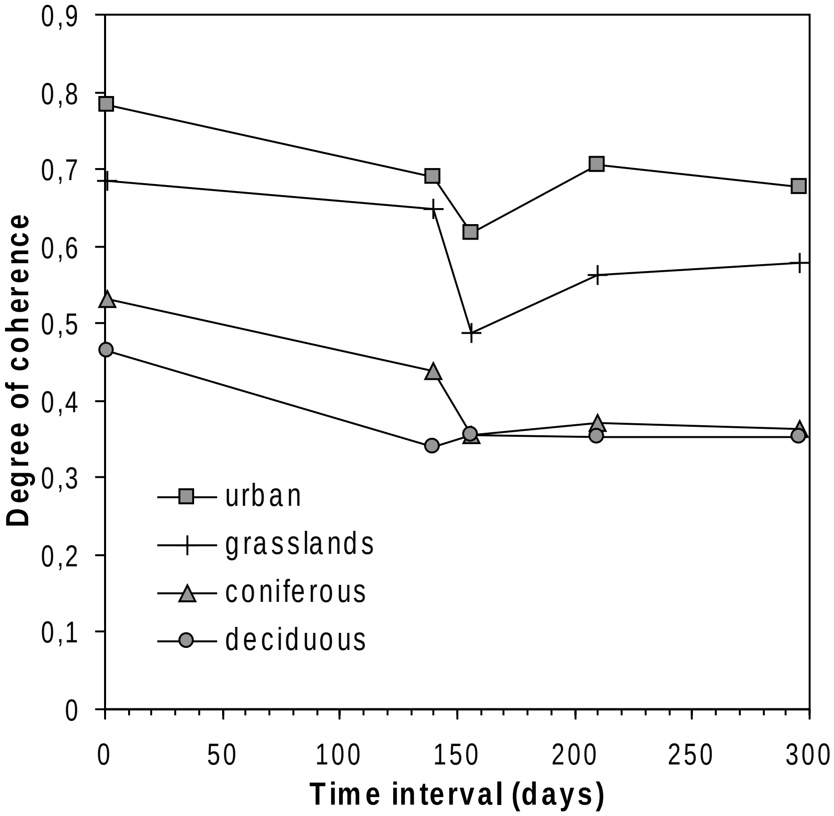

Mean correlation as a function of acquisition interval, for 4 main land-use types. All processed with DIAPASON

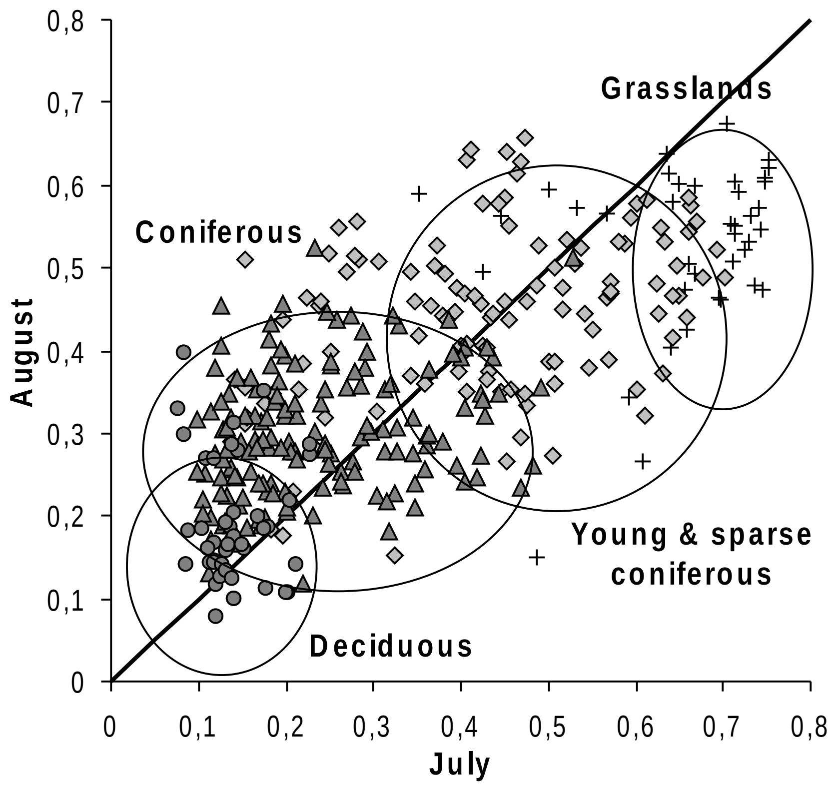

0,8
0,7
0,6
0,5
0,4
0,3
0,2
0,1
0
August
0
0,1
0,2
0,3
0,4
0,5
0,6
0,7
0,8
July
Grasslands
Coniferous
Young & sparse
coniferous
Deciduous

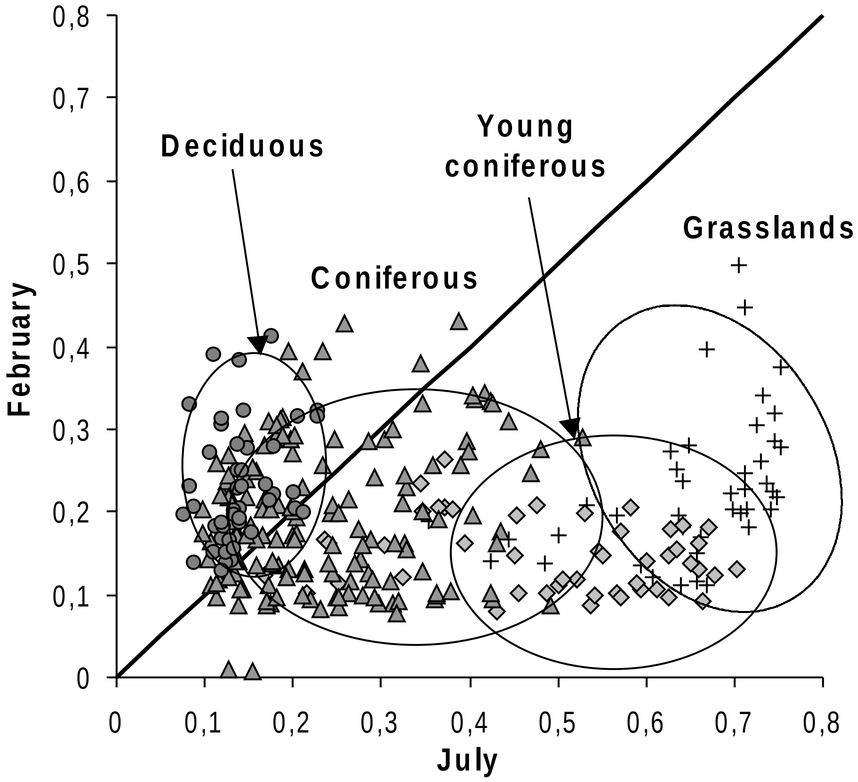
0,8
0,7
0,6
0,5
0,4
0,3
0,2
0,1
0
February
Deciduous
Young
coniferous
Grasslands
Coniferous
0
0,1
0,2
0,3
0,4
0,5
0,6
0,7
0,8
July

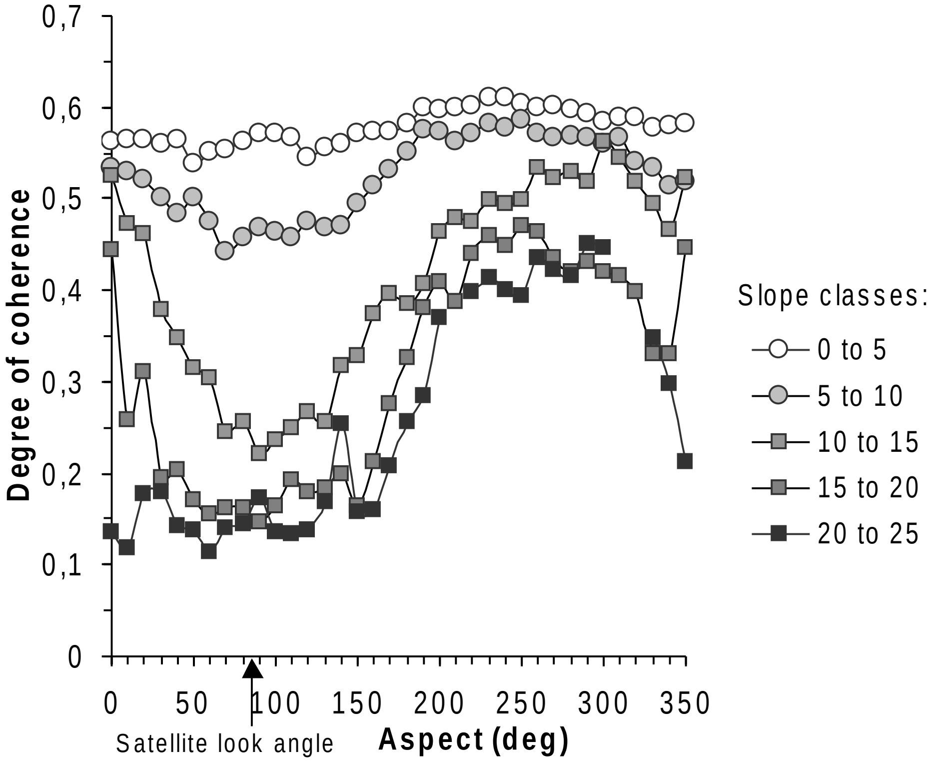

0,7
0,6
0,5
0,4
0,3
0,2
0,1
0
Degree of coherence
0
50
100
150
200
250
300
350
Satellite look angle
Aspect (deg)
Slope classes:
0 to 5
5 to 10
10 to 15
15 to 20
20 to 25

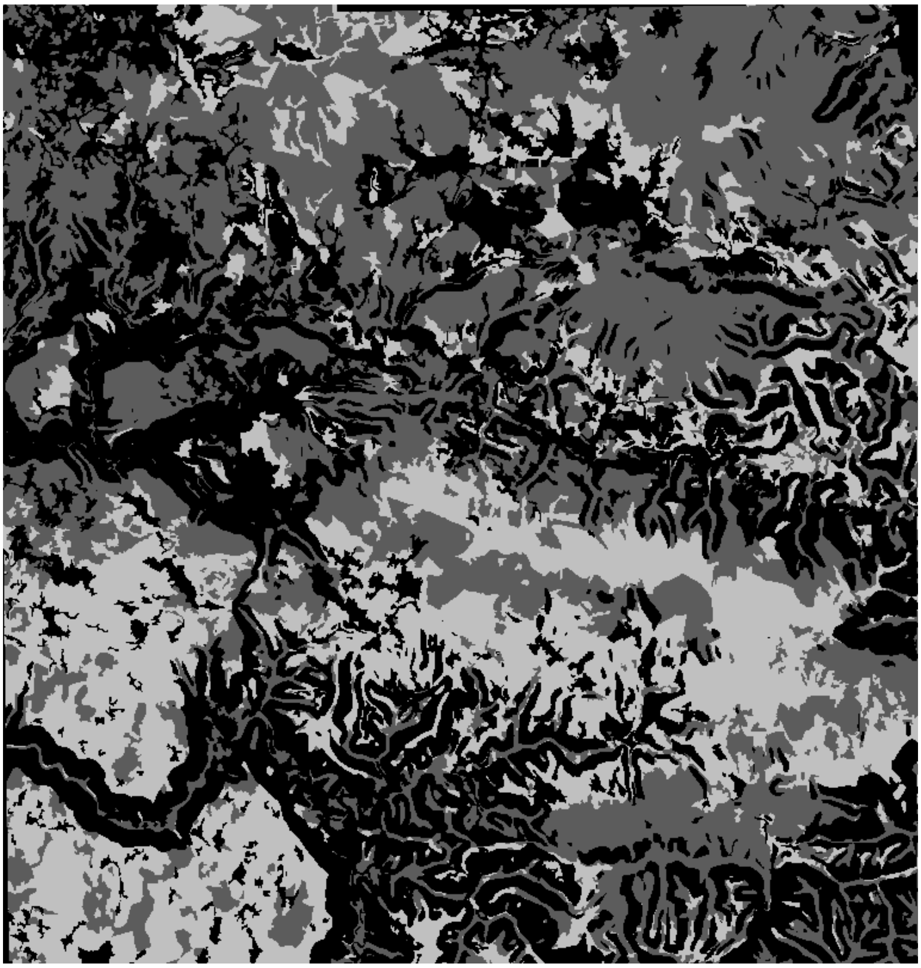

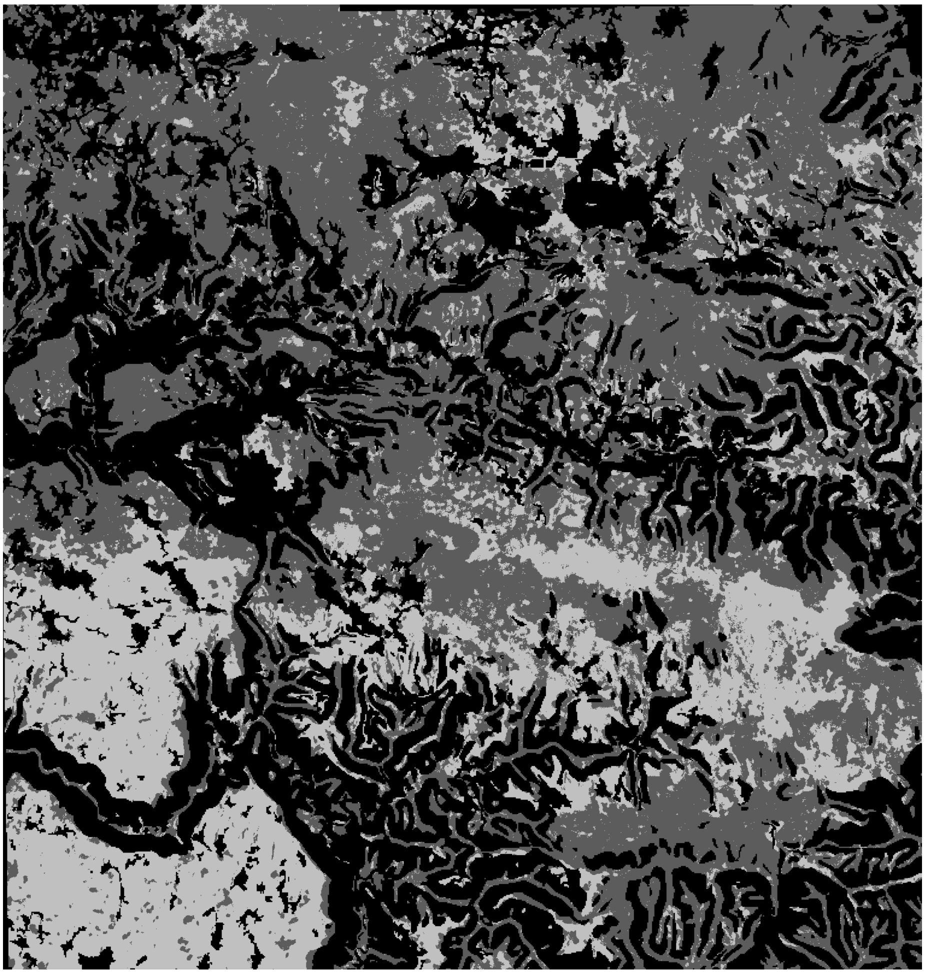

DIAPASON results — GAMMA results

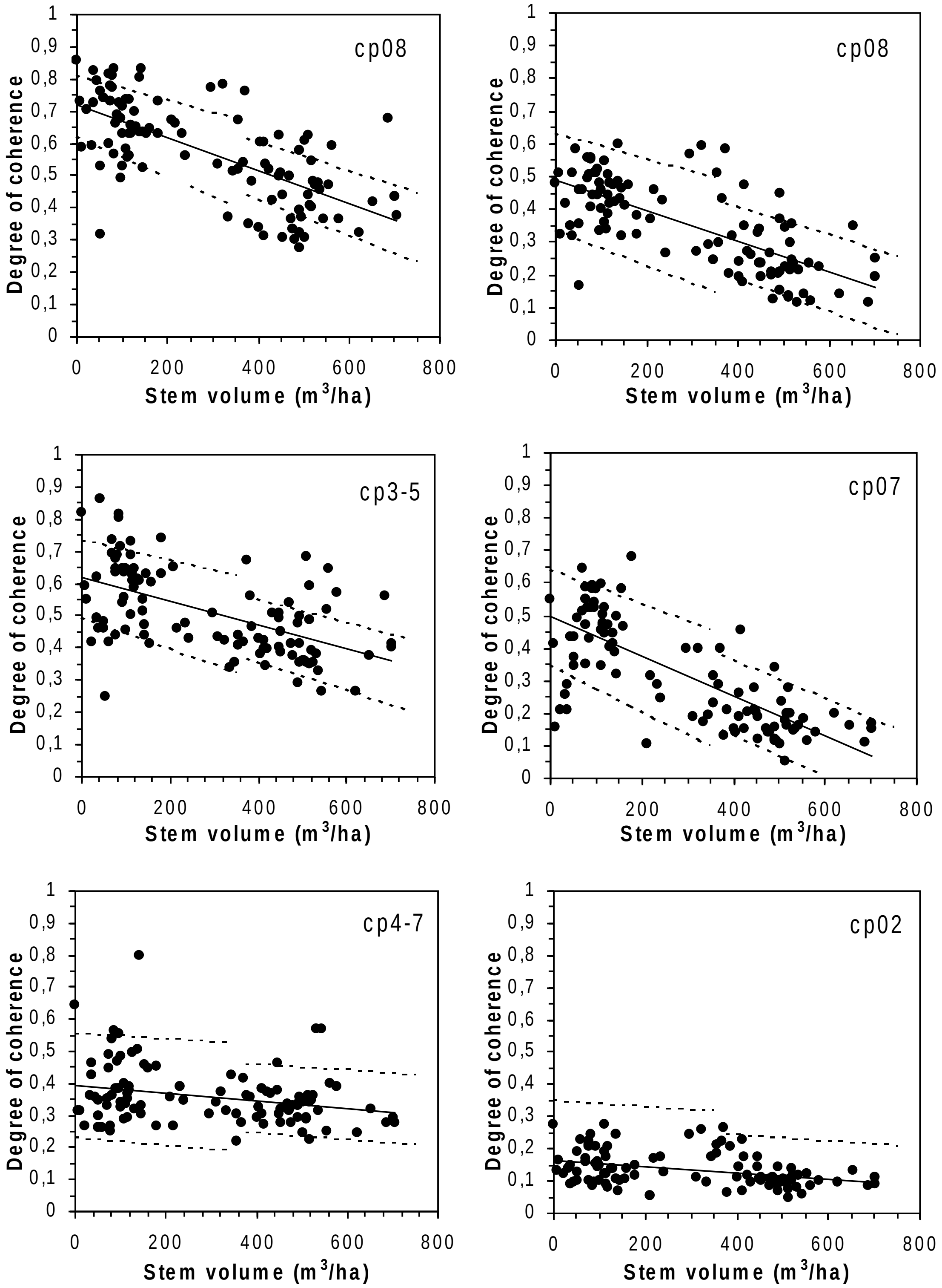

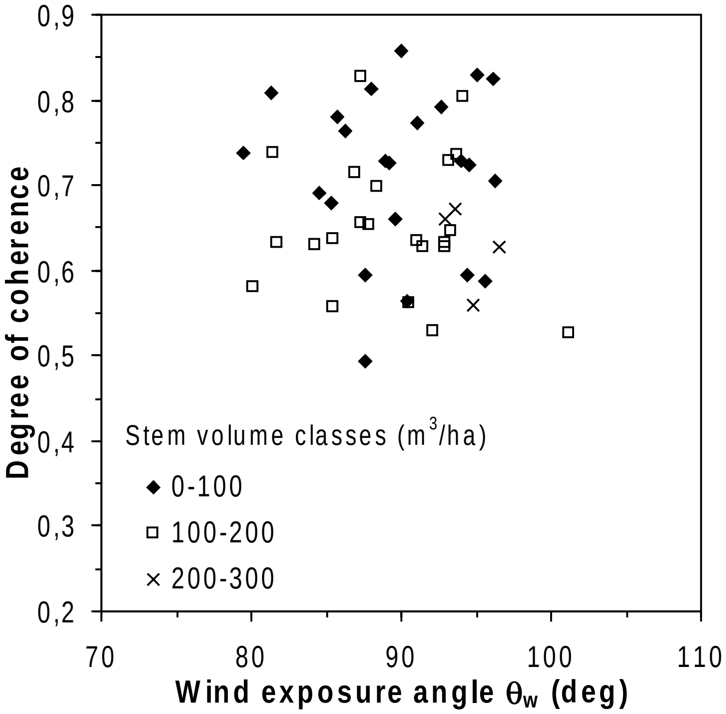
0,9
0,8
0,7
0,6
0,5
0,4
0,3
0,2
Degree of coherence
Stem volume classes (m3/ha)
0-100
100-200
200-300
70
80
90
100
110
Wind exposure angle θw (deg)

a)

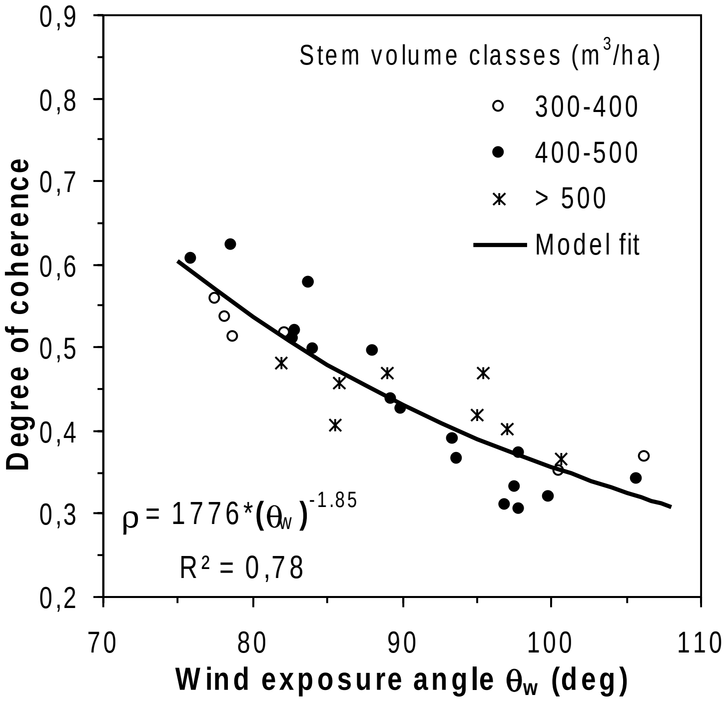
0,9
0,8
0,7
0,6
0,5
0,4
0,3
0,2
Degree of coherence
Stem volume classes (m3/ha)
300-400
400-500
> 500
Model fit
ρ = 1776*(θw)-1.85
R² = 0,78
70
80
90
100
110
Wind exposure angle θw (deg)

b)